International Journal of Chemical, Materials and Biomolecular Sciences
ISSN: 2415-6620
Vol:6, No:6, 2012

Application of Modified Maxwell-Stefan Equation for Separation of Aqueous Phenol by Pervaporation

Ujjal K Ghosh* and Ling Teen

***Abstract*—**Pervaporation has the potential to be an alternative to the other traditional separation processes such as distillation, adsorption, reverse osmosis and extraction. This study investigates the separation of phenol from water using a polyurethane membrane by pervaporation by applying the modified Maxwell-Stephen model. The modified Maxwell-Stefan model takes into account the non-ideal multi-component solubility effect, nonideal diffusivity of all permeating components, concentration dependent density of the membrane and diffusion coupling to predict various fluxes. Four cases has been developed to investigate the process parameters effects on the flux and weight fraction of phenol in the permeate values namely feed concentration, membrane thickness, operating temperature and operating downstream pressure. The model could describe semi-quantitatively the performance of the pervaporation membrane for the given system as a very good agreement between the observed and theoretical fluxes was observed.

***Keywords*—**Pervaporation, Phenol, Polyurethane, Modified Maxwell-Stefan equation, Solution Diffusion

I. Introduction

PHENOLIC compounds are by-products of many chemical, petroleum and pharmaceutical industries. Due to its toxic nature to human health, phenols are therefore required to be separated from the compound for safe disposal of the distillate. Phenol can then be recycled back as feed or be sold to other industries such as herbicide plants as a raw material [1]. According to Moraes et al. [2], the acceptable safe levels of phenol to be disposed of, as set by environmental laws, is 0.5 ppm, which makes traditional methods such as azeotropic distillation of phenol very difficult and energy consuming.

Membrane separation is one of the effective physicochemical methods that include microfiltration, ultrafiltration, reverse osmosis and pervaporation (PV). Compared with other traditional processes, pervaporation appeared far more effective due to its simplicity and high selectivity. Pervaporation with polymeric membranes of high perm selectivity were used for effective dehydration of alcohol, recovery of aromatic compounds and separation of organic solvents.

*Ujjal K Ghosh is with the Department of Chemical Engineering, School of Engineering and Science, Curtin University, CDT 250, 98009 Miri, Sarawak, Malaysia (phone: 60-85-443889; fax: 60-85-443837; e-mail: ujjal@curtin.edu.my).

Ling Teen is with the Department of Chemical Engineering, School of Engineering and Science, Curtin University, CDT 250, 98009 Miri, Sarawak, Malaysia.

Polyurethane membrane has a unique polymer chain structure and morphology comprising of rigid hard segment (diisocyanate and chain extender, viz., diol, diamine) and flexible soft segment (polyol). Polyether-based polyurethane membranes have been used for pervaporative separation of phenolic compounds from aqueous solution [3, 4]. Park and Chung [5] worked on removal of phenol from aqueous solution by liquid emulsion membrane. Park and co-workers documented mass transfer of phenol through supported liquid membrane [6].

The driving force of PV is the gradient in chemical potential of each component which can be accurately estimated by using Fick's law to calculate its flux. This gradient is normally created by maintaining a close to vacuum pressure on the permeate side thus, enabling the flux to be estimated by the partial pressure difference as well [7]. Pervaporative separation has the potential to improve the performance by combining with integrated systems or even replace the usage of the more conventional separation methods used today such as distillation, adsorption, reverse osmosis and extraction. But due to market barriers like the lack of information about PV, the poor availability of capital investments, scarce membrane market and the competition against other membrane separation techniques like nanofiltration and ultrafiltration, PV has not been able to develop as quickly as other methods. In this communication we report the simulation of the phenol-water separation by pervaporation using polyurethane (PU) membranes. The modified Maxwell-Stefan model was used to simulate the selected pervaporation system. The simulated results were found in agreement with existing literatures to determine its validity. The relationship between the factors affecting pervaporation and the feed and permeate flux will also be described in detail.

II. Transport Modeling through Dense Membrane

On a microscopic level, the PV process involves a sequence of five steps [8]: (1) selective sorption of liquid phase from its bulk into the membrane, (2) dissolution of the liquid into the membrane, (3) selective diffusion of the sorbed component through the membrane, (4) desorption of the sorbed fluid into vapor form at the permeate side, and (5) diffusion of the vapor permeate at the membrane surface into the bulk vapor. Fig.1 shows this.

A. Solution Diffusion Model

The solution-diffusion model (SDM) can be used to describe the mass transport of the component from feed side, through the membrane and finally to the permeate side. This model describes the pervaporation process in three steps: (1) sorption from liquid phase into membrane, (2) diffusion of the sorbed components through the membrane, and (3) desorption from the membrane into the vapor phase at the permeate side [7, 9].

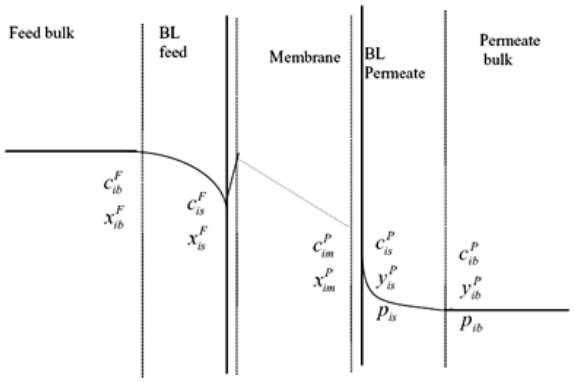

Fig. 1 Mass transport steps during pervaporation

The model is under the assumption that the membrane's pressure is constantly uniform and the chemical potential gradient across the membrane is expressed only as an concentration gradient. This assumption then also indirectly assumes that the membrane transfers pressure in a similar way as liquids [9]. Based on the assumptions above, the pressure gradient or flux, J (g m^{-2}h^{-1}) of the permeation can be expressed as [7]:

$$J = \frac{Q}{A\,t} \tag{1}$$

Flux, J is defined as the quantity of the high affinity component towards the membrane permeated per unit time. Q is the weight of permeate of either phenol, water or both components while A (m^2) and t (h) represent the effective membrane area and time period, respectively.

Perm-selectivity or the separation factor for permeation, α is a parameter which assesses the performance of a membrane and it is generally expressed by [7]:

$$\alpha = \frac{c_{i2}}{c_{i1}}\frac{c_{j1}}{c_{j2}} \tag{2}$$

where C (g m^{-3}) denotes the concentration on the feed (1) and the permeate (2) sides for components i and j. Activation energy, E_J (kJ mol^{-1}) of pervaporation can be calculated using the modified Arrhenius equation where when plotted, the slope is the activation energy value [4, 7].

$$J_i = J_{i,o}\exp\left(\frac{-E_j}{RT}\right) \tag{3}$$

where gas constant, R = 8.314 J K^{-1} mol^{-1} and T denotes feed liquid temperature in K.

B. Modified Maxwell-Stefan Model

The transport through a membrane for pervaporation (PV) can also be sufficiently modeled by Maxwell-Stefan equations and was derived based on the SDM. This model had been further generalized by Mason and Viehland [10] by applying the basic principles of statistical mechanics and the classical-mechanical Liouville equation. For the relationship between chemical potential driving force and friction resistance in a multi-component solution, it was expressed as:

$$\frac{d\mu_i}{dz} = \sum_{j=1}^{n} x_j (v_j - v_i)\frac{RT}{D_{ji}^o} \tag{4}$$

where $d\mu_i/dz$ is the chemical potential gradient of component i, x_j is the mole fraction of j components where j = 0, 1, 2, …, n. v represents the local velocities of the components and $RT/\ D_{ji}^o$ represents the frictional effect exerted by component j on i.

Flux equations for three components, which include a binary mixture and membrane, can be expressed in equations (5) and (6) below [9]:

$$J_1 = \overline{D}_{1,M}\left(\frac{\overline{D}_{2,M}\overline{w}_1^{/} + D_{12}}{D_{12} + \overline{D}_{2,M}\overline{w}_1^{/} + \overline{D}_{1,M}\overline{w}_2^{/}}\right)\overline{\rho}_M\frac{\Delta\overline{w}_1^{/}}{l} + \overline{D}_{1,M}\left(\frac{\overline{D}_{2,M}\overline{w}_1^{/}}{D_{12} + \overline{D}_{2,M}\overline{w}_1^{/} + \overline{D}_{1,M}\overline{w}_2^{/}}\right)\overline{\rho}_M\frac{\Delta\overline{w}_2^{/}}{l} \tag{5}$$

$$J_2 = \overline{D}_{2,M}\left(\frac{\overline{D}_{1,M}\overline{w}_2^{/} + D_{12}}{D_{12} + \overline{D}_{2,M}\overline{w}_1^{/} + \overline{D}_{1,M}\overline{w}_2^{/}}\right)\overline{\rho}_M\frac{\Delta\overline{w}_2^{/}}{l} + \overline{D}_{2,M}\left(\frac{\overline{D}_{1,M}\overline{w}_2^{/}}{D_{12} + \overline{D}_{2,M}\overline{w}_1^{/} + \overline{D}_{1,M}\overline{w}_2^{/}}\right)\overline{\rho}_M\frac{\Delta\overline{w}_1^{/}}{l} \tag{6}$$

where $\overline{w}_i^{/} = (w_{iF}^{/} + w_{iP}^{/})/2$ *and* $\Delta\overline{w}_i^{/} = w_{iF}^{/} - w_{iP}^{/}$.

$w_i^{/}$ is the weight fraction of components 1 and 2 in a membrane, $\overline{\rho}_M$ is the mean density of the swollen membrane and D_{iM} is the diffusion coefficients of component 1 and 2 in the membrane respectively. The average diffusion coefficient of a pure component in the active layer of the membrane, D_{iM} and the averaged density of a polymer membrane, $\overline{\rho}_M$ are defined as:

$$\overline{D}_{i,M} = \frac{\int_{w_{iP}^{/}}^{w_{iF}^{/}} D_{i,M}(w_i^{/})dw_i^{/}}{w_{iF}^{/} - w_{iP}^{/}} \tag{7}$$

$$\overline{\rho}_M = \frac{\int_{w_{iP}^{/}}^{w_{iF}^{/}} \rho_M(w_i^{/})dw_i^{/}}{w_{iF}^{/} - w_{iP}^{/}} \tag{8}$$

III. Polyurethane Membrane Properties

To fully understand the transport behavior of the separation of phenol and water through the polyurethane (PU) membrane, it is important to look into the properties of the membrane itself as well.

The PU membrane properties for this work had been determined as follows:

- Non-porous;
- It is hydrophobic, thus, it has selectivity towards phenol [4];

- Its structure is of a unique combination of a hard section which is moderately polar and a soft section which is non polar. This occurs as the blocks undergo microphase separation due to their thermodynamic incongruity. The hard sections are impermeable while the soft sections are permeable [11]. Fig.2 shows the typical structure of PU;
- The ratio of soft segments to hard segments can be altered by adjusting the mole ratios of the reagents when synthesizing the membrane and the length of soft segments can be controlled by the type of macrodiol relative molecular mass [12]. Theoretically, by increasing the soft-segments, the degree of phase separation will increase as well but to what extent, still needs more experimentation works.

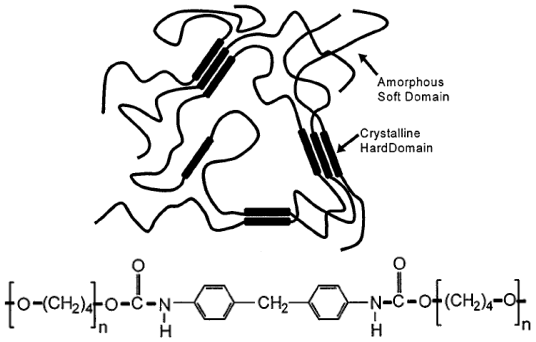

Fig. 2 Polyurethane membrane structure

IV. Simulation Methodology using Modified Maxwell-Stefan Model

Four different cases with a different manipulated variable were simulated:

- Effect of phenol concentration in feed with constant temperature of 60°C, downstream pressure of 2.50mmHg and membrane thickness of 1×10^{-6} m.
- Effect of membrane thickness with constant temperature of 60°C, downstream pressure of 2.50mmHg and 1wt% of phenol feed.
- Effect of system temperature with constant downstream pressure 2.5mmHg, 1wt% of phenol feed and membrane thickness of 1×10^{-6} m.
- Effect of downstream pressure with constant temperature of 60°C, 1wt% of phenol feed and membrane thickness of 1×10^{-6} m.

The effects of the manipulated variable as mentioned above will be evaluated based on the partial flux calculation results using modified Maxwell-Stefan pervaporation model. In order to calculated this, input data namely concentration dependence of density of a membrane, concentration dependence of the diffusion coefficients of pure components in the membrane, weight fractions of the components in the feed and permeate, coupled diffusion coefficient and the thickness of the membrane is required. For the phenol-water pervaporation through a PU membrane, the required data was obtained from [13] as displayed in the subsequent subsections in this chapter. The membrane thickness for the data obtained is not available and thus, estimations of the value will be made accordingly and justified. The membrane density has been assumed to be 950 kg m^{-3} throughout all the simulation cases [4]. This is so that the effect of the manipulated variable can be more distinct and a clearer comparison between each of the cases can be done.

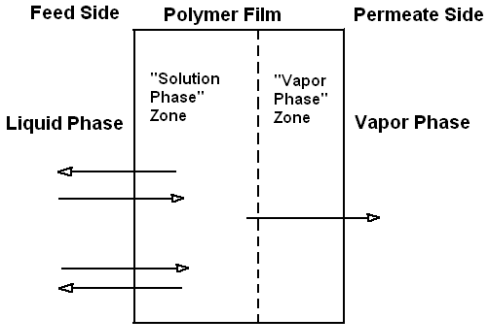

Fig. 3 Solution and vapor phase zones in a membrane

A. Simulation Methodology with Data Extraction

A swollen membrane consists of two zones namely the 'solution phase' and the 'vapor phase' zone as shown in Figure 3 and obtaining the weight fractions of phenol and water for the two zones respectively, is the first step to simulating the flux behavior based on the modified Maxwell-Stefan model. Weight fraction of phenol and water within the membrane in the solution zone, $\overline{w}_{iF}^{l}$, was obtained from Hoshi et al. [13] directly.

The diffusion coefficients for both components were also obtained from the paper directly but the diffusion coupling coefficient, D_{12} is not available. Based on [4], it was observed that D_{12} lies between the D_1 and D_2 coefficients. Hence another assumption was made here, whereby, the D_{12} is an average of the other two coefficients. With this, the data collection is complete and the flux and new phenol in permeate percentage values was calculated based on the equations stated above. Table 1 shows the collected data based on the conditions for Case 1.

The assumption made to estimate the D_{12} coefficient are made instead of simply extracting the existing data in literature because of the different operating conditions that the system is running at as well as the different composition of phenol-water solution used which may deviate the results. Estimating the value would then ensure that the generated results are as consistent as possible to the data extracted from Hoshi et al. [13], which is limited by the accuracy of the assumptions made.For Case 2, all the data required was taken from Table 1 when the phenol in feed is 1wt%. It is assumed that the diffusion coefficients are the same for all the different membrane thicknesses for ease of calculation. The partial fluxes and the calculated phenol in permeate percentage was then calculated for thicknesses of 2, 5, 8, 10, 20, and 50μm respectively.

TABLE I
EFFECT OF PHENOL CONCENTRATION ON PERVAPORATION (DATA EXTRACTED FROM [13])

Phenol in Feed (wt%)	0.5	1	3	5	7
Phenol in permeate (wt%)	21	28	54	63	65
$\overline{w}_{1F}^{/}$	0.61	0.67	0.75	0.65	0.81
$\overline{w}_{2F}^{/}$	0.39	0.33	0.25	0.35	0.19
$\overline{w}_{1P}^{/}$	0.0006	0.0019	0.0122	0.0204	0.0366
$\overline{w}_{2P}^{/}$	0.3055	0.2352	0.1107	0.1241	0.0627
D_1 ($\times 10^{12}$ m^2s^{-1})	0.28	0.60	1.80	2.70	5.80
D_2 ($\times 10^{12}$ m^2s^{-1})	2.20	2.50	3.80	3.00	12.0
D_{12} ($\times 10^{12}$ m^2s^{-1})	1.24	1.55	2.80	2.85	8.90

The diffusion coupling coefficient is not available and was estimated based on the D_{12} trend observed in [4]. It is found that the coefficient increases rather steadily when the temperature increases. From here, the assumption that with every 10°C temperature increment, the coefficient increases by 20% with D_{12} at 60°C as the basis while ensuring that the value still falls between the D_1 and D_2 values. The D_{12} value at 60°C is again obtained from the previous estimation shown in Table I. Table II shows the extracted data for Case 3.

TABLE II
EFFECT OF SYSTEM TEMPERATURE ON PERVAPORATION (DATA EXTRACTED FROM [13])

Temperature (°C)	**50**	**60**	**70**	**80**
Phenol in permeate (wt%)	26	28	29	28
$\overline{w}_{1F}^{/}$	0.61	0.67	0.65	0.7
$\overline{w}_{2F}^{/}$	0.39	0.33	0.35	0.3
$\overline{w}_{1P}^{/}$	0.0016	0.0019	0.0019	0.002
$\overline{w}_{2P}^{/}$	0.2857	0.2352	0.246	0.2138
D_{12} ($\times 10^{13}$ m^2s^{-1})	12.4	15.5	18.6	21.7

Extracted data for Case 4 is summarized in Table 3. Values which are constant for all downstream pressures are D_{12}, w'_{1F} and w'_{2F} at 60°C and 1wt% phenol feed which can be obtained from Table 1 once again. For this case, the phenol in permeate data is not available from Hoshi et al. [13]. Thus, an assumption that the phenol vapor in the permeate is in equilibrium with the vapor phase zone in the membrane. Therefore the $\overline{w}_{1F}^{/}$ value is directly obtained from the phenol in permeate literature value.

TABLE III
EFFECT OF DOWNSTREAM PRESSURE TEMPERATURE ON PERVAPORATION (DATA EXTRACTED FROM [13])

P (mmHg)	**0.5**	**2.5**	**5**	**10**	**20**	**30**
Phenol in permeate (wt%)	28	28	26	20	10	7
$\overline{w}_{1P}^{/}$	0.28	0.28	0.26	0.20	0.10	0.07
$\overline{w}_{2P}^{/}$	0.72	0.72	0.74	0.80	0.90	0.93

V. RESULTS AND DISCUSSION

A. Effect of Feed Concentration

When the feed concentration increases for an aqueous mixture, the permeation flux increases because the driving force for mass transfer increases. The increase can also be attributed by the plasticizing effects of certain solutes such as phenol, by the increase of its concentration [8]. Table 4 depicts the simulated results as a function of feed phenol concentration. It is observed that both fluxes increase from 178.48 to 6359.09 g $m^{-2}h^{-1}$ and 217.76 to 792.22 g $m^{-2}h^{-1}$, respectively, as the feed phenol concentration increases from 0.5 to 7 wt%. It can also be seen from Table 4 that the phenol partial flux increases at a faster rate. This can be attributed to the penetration of phenol molecules at a higher rate when the feed concentration is higher; thereby the phenol diffusivity is higher than that of water's diffusion rate.

TABLE IV
SIMULATED RESULTS – EFFECT OF FEED PHENOL CONCENTRATION

Phenol in Feed, wt%	**0.5**	**1**	**3**	**5**	**7**
$\Delta\overline{w}_1^{/}$	0.6094	0.6681	0.7378	0.6296	0.7734
$\Delta\overline{w}_2^{/}$	0.0845	0.0948	0.1393	0.2259	0.1273
$\overline{w}_1^{/}$	0.3053	0.3359	0.3811	0.3352	0.4233
$\overline{w}_2^{/}$	0.3477	0.2826	0.1804	0.237	0.1264
$\overline{D}_{1M}$ ($\times 10^{13}$ m^2s^{-1})	0.855	2.02	6.86	9.05	24.6
$\overline{D}_{2M}$ ($\times 10^{13}$ m^2s^{-1})	7.65	7.07	6.85	7.11	15.2
J_1 (gm^{-2} h^{-1})	178.48	454.75	1690.48	1872.66	6359.09
J_2 (gm^{-2} h^{-1})	217.76	250.74	381	624.04	792.22
Phenol in permeate, calc (%)	45	64	82	75	89

The phenol concentration in permeate increases from 45% to 89%. The increment at feed concentrations 0.5 to 3 wt% is sharper than the increment at feed concentrations more that 3wt%. This can be explained by the swelling of the membrane. Higher feed concentration causes the membrane to swell more and expand in thickness. This expansion and the extra molecules in the membrane in turn results in an increased difficulty for diffusion. Depending on the stability of the membrane, there is only a certain upper limit that the feed concentration can be increased to because the high concentration will cause the membrane to swell over its limit and start to dissolve [14] of which cannot be modeled by the Maxwell-Stefan model.

B. Effect of Membrane Thickness

Membrane thickness has an inverse relationship with the permeation rate. This trend can be seen in Table 5 where the phenol and water partial fluxes decrease from 227.38 to 9.10 g $m^{-2}h^{-1}$ and 125.37 to 5.02 g $m^{-2}h^{-1}$, respectively, with a sharp drop in the phenol flux at 5μm. This is because the thickness of the membrane and the swelling poses as a flow resistance to the permeate. Therefore, it is desirable to use thin films to minimize the resistance. Normally, the membrane support plate that the membrane rests on also creates a resistance. By designing the backing plate to be porous, that resistance is normally assumed to be negligible.

The phenol in the permeate calculation results for all membrane thickness in this case is calculated to be 65%. This is an error as the percentage is supposed to slightly increase as documented in Hoshi et al. [13]. This error can be accounted for by the assumption that the diffusion coefficients D_1, D_2 and

D_{12} were assumed to be the same for all membrane thicknesses when in practice, the flow resistances that caused the decrease in flux mentioned before, will also cause the diffusion coefficients to change.

TABLE V
SIMULATED RESULTS – EFFECT OF MEMBRANE THICKNESS

Membrane Thickness (μm)	2	5	8	10	20	50
J_1 (gm^{-2} h^{-1})	227.38	90.95	56.84	45.48	22.74	9.10
J_2 (gm^{-2} h^{-1})	125.37	50.15	31.34	25.07	12.54	5.02
Phenol in permeate, calc (%)	65	65	65	65	65	65

C.Effect of System Temperature

The effect of temperature on partial fluxes was studied in the temperature range of 50 to 80°C. An increase in feed temperature usually causes an increase permeation rate and a decrease in membrane selectivity. This is because the temperature excites the polymer at a molecular level, increasing its frequency and amplitude of motion which causes the polymer to unfold its chains, creating a larger free volume for permeation to occur. The membrane selectivity usually decreases because the unfolded chains of the polymer membrane allow both the permeation of the organic compound and water [15].

TABLE VI
SIMULATED RESULTS – EFFECT OF FEED TEMPERATURE

Temperature (°C)	50	60	70	80
$\Delta\overline{w}_1^{/}$	0.6084	0.6681	0.6481	0.698
$\Delta\overline{w}_2^{/}$	0.1043	0.0948	0.104	0.0862
$\overline{w}_1^{/}$	0.3058	0.3359	0.3259	0.3510
$\overline{w}_2^{/}$	0.3379	0.2826	0.2980	0.2569
$\overline{D}_{1M}$ ($\times 10^{13}$ m^2s^{-1})	1.83	2.02	1.96	2.11
$\overline{D}_{2M}$ ($\times 10^{13}$ m^2s^{-1})	8.45	7.07	7.45	6.42
J_1 (gm^{-2} h^{-1})	377.44	454.75	429.61	497.34
J_2 (gm^{-2} h^{-1})	320.07	250.74	280.38	207.25
Phenol in permeate, calc (%)	54	65	61	71

Comparing the results from Ghosh and co-workers [4], it can be confirmed that a phenol-water system behaves in this manner. However, the simulated results (Table 6) show that the partial flux of phenol increases from 377.44 to 497.34$gm^{-2}h^{-1}$. As for the newly calculated phenol in permeate percentage, the results shows a steady increase as there is an increase in the phenol flux. The increment, however, should not have such a big range of 54 to 71% because the water flux should have slightly increased as well. Therefore, from the results, it was determined that a higher temperature is more advantageous when recovering the solute, but only to a certain degree. High temperatures can cause the membrane to dissolve and degrade [8], which in this case, was not successfully modeled, due to the water partial flux error.

D.Effect of Downstream Pressure

From Table VII, it can be seen that the difference in weight fraction in membrane, $\Delta\overline{w}_1^{/}$, yields a negative value. This situation occurred as the assumption made for the vapor zone phenol concentration in the membrane does not take into account the fraction of the water which did not diffuse through and remained in the retentate. To overcome this, the negative is ignored.

The effect of permeate side pressure on the fluxes is shown in Table VII. It can be observed that as the downstream pressure increases, the water flux decreases more drastically than phenol, from 617.98 to 135.52$gm^{-2}h^{-1}$ whereas, the phenol partial flux decreases from 176.59 to 35.45$gm^{-2}h^{-1}$. The pervaporation driving force is based in the chemical potential difference of the feed and permeate side which can be achieved by means of applying vacuum on the permeate side and as the downstream pressure decreases, the permeation rate would increase. This phenomenon may also be explained by the membrane's polymeric structure that has a greater resistance to the fluxes and require lower pressures for a higher permeation of phenol.

TABLE VII
SIMULATED RESULTS – EFFECT OF PERMEATE PRESSURE

P (mmHg)	0.5	2.5	5	10	20	30
$\Delta\overline{w}_1^{/}$ [a]	-0.2661	-0.27	-0.2464	-0.19	-0.09	-0.0567
$\Delta\overline{w}_2^{/}$	0.2661	0.27	0.2464	0.19	0.09	0.0567
$\overline{w}_1^{/}$	0.1431	0.1450	0.1332	0.1050	0.0550	0.0383
$\overline{w}_2^{/}$	0.8569	0.8550	0.8668	0.8950	0.9450	0.9617
$\overline{D}_{1M}$ ($\times 10^{13}$ m^2s^{-1})	2.02	2.02	2.02	2.02	2.02	2.02
$\overline{D}_{2M}$ ($\times 10^{13}$ m^2s^{-1})	7.07	7.07	7.07	7.07	7.07	7.07
J_1 (gm^{-2} h^{-1})	176.59	179.35	162.66	123.51	56.87	35.45
J_2 (gm^{-2} h^{-1})	617.98	626.65	573.78	445.91	214.22	135.52
Phenol in permeate, calc (%)	22	22	22	21	20	20

[a] Negative value ignored for flux calculations

As for the simulated results for the percentage of phenol in the permeate, comparing with the experimental data from Hoshi et al. [13] and Moraes et al. [2], the results should have shown quite a sharp decrease in the phenol in the permeate but this is not the case. The results tabulated as Table 7 shows that the value is relatively unchanged, from 22 to 20%. This error can again be accounted for diffusion coefficient assumption made as explained earlier.

VI. CONCLUSION

The modified Maxwell-Stefan model takes into account the non-ideal multi-component solubility effect, nonideal diffusivity of all permeating components, concentration dependent density of the membrane and diffusion coupling to predict various fluxes. In conclusion, the Maxwell-Stefan model can accurately simulate the pervaporation separation process of phenol and water. Results showed that when the phenol in the feed increases, the partial fluxes of the phenol and water also increases but with the former having a more drastic increment. The effect of membrane thickness on the fluxes, however, is inversely proportional, where the thick membrane creates a greater resistance for the diffusion of the components to the permeate side. The same goes for the

increase of the downstream pressure. As for the effect of the system temperature, the simulated results are also in line with the compared literature values. There are some errors however, which were primarily caused by the assumed diffusion coefficient values.

NOMENCLATURE

A Effective membrane area, m^2
C_{i1} Concentration of component i in feed, g m^{-3}
C_{i2} Concentration of component i in permeate, g m^{-3}
C_{j1} Concentration of component j in feed, g m^{-3}
C_{j2} Concentration of component j in permeate, g m^{-3}
D_i Diffusion coefficient of component i, m^2 s^{-1}
D_{iM} Average diffusion coefficient of pure component i in membrane phase, m^2 s^{-1}
E_J Activation energy of permeation, kJ mol^{-1}
J Permeate flux, g m^{-2} s^{-1}
J_i Permeate flux for component i, g m^{-2} s^{-1}
J_{io} Pre-exponential factor for permeate flux for component i, g m^{-2} s^{-1}
l Thickness of membrane, m
Q Weight of permeate, g
t Time of permeation, s
T Temperature in absolute scale, K
w_{1F} Weight fraction of component 1 in feed
w_{1P} Weight fraction of component 1 in permeate
w_1' Weight fraction of component 1 in membrane phase
x_j Mole faction of component j

Greek Letters
α Separation factor
δ_M Thickness of membrane
μ_i Chemical potential of component i
ν_j Local velocity of component j, m s^{-1}

REFERENCES

[1] E. El-Zanati, E. Abdel-Hakim, O. El-Ardi and M. Fahmy, “Modeling and simulations of butanol separation aqueous solutions using pervaporation”, Journal of Membrane Science, vol. 280, pp.278-283, 2006.
[2] E. B. Moraes, M.E.T. Alvarez, F.R. Perioto and M.R. Wolf-Marciel n.d., “Modeling and simulation for pervaporative process: an alternative for removing phenol from wastewater”, http://www.aidic.it/icheap9/webpapers/285Moraes.pdf
[3] T. Gupta, N. C. Pradhan and B. Adhikari, “Separation of Phenol from Aqueous solution by pervaporation using HTPB based polyurethaneurea membrane”, Journal of Membrane Science, vol. 217, pp. 43-53, 2003.
[4] U. K. Ghosh, N. C. Pradhan and B. Adhikari, “Separation of Water and o-Chlorophenol by Pervaporation using HTPB-based Polyurethaneurea Membranes and Application of Modified Maxwell-Stefan Equation”, Journal of Membrane Science, vol. 272, pp. 93-102, 2006.
[5] H-J. Park and T-S. Chung, “Removal of Phenol from Aqueous Solution by Liquid Emulsion Membrane”, Korean Journal of Chemical Engineering, vol. 20, pp. 731-735, 2003.
[6] S. W. Park, C. F. Kaseger, J. K. Moon and J. H. Kim, “Mass transfer of phenol through supported liquid membrane”, Korean Journal of Chemical Engineering, vol. 13, pp. 596-605, 1996.
[7] U. K. Ghosh, N.C. Pradhan and B. Adhikari, “Pervaporative Recovery of N-Methyl-2-pyrrolidone from Dilute Aqueous Solution ”, Journal of Membrane Science, vol. 285, pp. 249-257, 2006.
[8] J. G. Wijimans and R. W. Baker, “The solution-diffusion model: a review”, Journal of Membrane Science vol. 107, pp. 1-21, 1995.
[9] P. Izak, L. Bartovska, K. Friess, M. Sipek, and P. Uchytil, "Description of binary liquid mixtures transport through non-porous membrane by modified Maxwell-Stefan equations", Journal of Membrane Science, vol. 214, pp. 293-309, 2003.
[10] E. A. Mason, and L. A. Viehland., Journal of Chemical Physics, vol., 68, pp. 3562, 1978.
[11] M. E. McComb, R. D. Oleschuk, D. M. Manley et al., “"Use of a Non-porous Polyurethane Membrane as a Sample Support for Matrix-assisted Laser Desorption/Ionisation Time-of-flight Mass Spectronomy of Peptides and Proteins”, Rapid Communications in Mass Spectronomy II, 1716-1722, 1997.
[12] A. Wolinska-Grabczyk, J. Muszynski, and A. Jankowski, "Applications of Polyurethane-Based Membranes in Pervaporation Separations”, Chem. Papers, vol. 54, pp. 389, 2000.
[13] M. Hoshi, M. Kogure, T. Saitoh and T. Nakagawa, "Separation of Aqueous Phenol through Polyurethane Membranes by Pervaporation." Journal of Applied Polymer Science, vol. 71, pp. 469, 1997.
[14] F. Pithan and C. Staudt-Bickel, “Crosslinked copolymide membranes for phenol recovery from process water by pervaporation”, Chemphyschem, vol. 4, pp. 967, 2003.
[15] M. Peng, L. M. Vane and S. X. Liu, “Recent advances in VOCs removal from water from pervaporation”, Journal of Hazardous Materials, vol. 98, pp. 69, 2003.